Preprint YERPHI-1288(74)-90

ԵՐԵՎԱՆԻ ՖԻԶԻԿԱՅԻ ԻՆՍՏԻՏՈՒՏ
ЕРЕВАНСКИЙ ФИЗИЧЕСКИЙ ИНСТИТУТ
YEREVAN PHYSICS INSTITUTE

F.A.AHARONIAN, B.L.KANEVSKY, V.A.SAHAKIAN

ON SOME PECULIARITIES OF EAS INITIATED BY GAMMA-RAYS OF EXTREMELY HIGH ENERGIES

YEREVAN 1990

ЦНИИатоминформ
ЕРЕВАН-1990

Նախնական հրատ. 1-38(74)-90

Ֆ.Ա. ԱՇԱՐՈՆՅԱՆ, Բ.Լ. ԿԱՆԵՎՍԿԻ, Ժ.Ա. ՍԱՀԱԿՅԱՆ

ՍԱՀՄԱՆԱՅԻՆ ՄԵԾ ԷՆԵՐԳԻԱՆԵՐԻ ԳԱՄԱ-ՔՎԱՆՏՆԵՐԻՑ ԱՌԱՋԱՑԱԾ ԼՄՀ-ՆԵՐԻ ՈՐՈՇ ԱՌԱՆՁՆԱՀԱՏԿՈՒԹՅՈՒՆՆԵՐԻ ՄԱՍԻՆ

Աշխատանքում հետազոտվում է սահմանային մեծ էներգիաների գամա-քվանտներից առաջացած ԼՄՀ-ում փոքր էներգիաների ($E_\mu \leq 1$ԳԷՎ) մյուոնների քանակը: Ցույց է տրված, որ մեծ խորությունների վրա ($\sim 10^{3}$ գ/սմ^2) $E_0 \sim 10^{18}$ էՎ էներգիայով գամա-քվանտներից առաջացած ԼՄՀ-ում փոքր էներգիայի մյուոնների քանակը նույն կարգի է, ինչ որ պրոտոնից առաջացած ԼՄՀ-ում, ի տարբերություն $E_0 \sim 10^{15}$ էՎ էներգիայի տիրույթի, որտեղ գամա-հեղեղները «մյուոնազուրկ» են: Հետազոտվում է Լանդաու-Պոմերանչուկ-Միգդալ էֆեկտի և գեոմագնիսական դաշտի հետ առաջնային ֆոտոնի փոխազդեցության ապրնցությունը էլեկտրամագնիսական հեղեղի զարգացման բնույթի վրա, $E_0 \geq 10^{19}$ էՎ էներգիանների դեպքում: Չի կարելի հաշվի չառնել այդ էֆեկտները սահմանային մեծ էներգիաների ԼՄՀ տվյալները բացատրելիս, եթե առաջնային տիեզերական ճառագայթման մեջ գամա-քվանտների պարունակությունը մեծ է ($\gamma/p > 0.1$):

Երևանի ֆիզիկայի ինստիտուտ

Երևան 1990

Preprint YERPHI-1288(74)-90

F.A.AHARONIAN, B.L.KANEVSKY, V.A.SAHAKIAN

ON SOME PECULIARITIES OF EAS INITIATED BY GAMMA-RAYS OF EXTREMELY HIGH ENERGIES

The number of low-energy muons ($E_\mu \leq 1$GeV) in EAS initiated by primary gamma-rays of extremely high energies is calculated. It is shown that at large depths ($s \geq 1000 g/cm^2$) the number of low-energy muons in EAS from gamma-rays with energy $E_0 \geq 10^{18}$eV is of the same order as in the proton-induced shower, as opposed to the energy range $E_0 \sim 10^{15}$eV, where the gamma-showers are "muon-poor". The influence of the Landau-Pomeranchuk-Migdal effect and of the interaction of the primary photon with the geomagnetic field on the development of an electromagnetic shower in the Earth's atmosphere at energies $E_0 \geq 10^{19}$eV is investigated. In case of a high content of gamma-rays in the primary cosmic radiation ($\gamma/p > 0.1$) one should not ignore these effects when interpreting data on EAS of extremely high energies.

Yerevan Physics Institute
Yerevan 1990

Препринт ЕрФИ-1288(74)-90

Ф.А. АГАРОНЯН, Б.Л. КАНЕВСКИЙ, В.А. СААКЯН

О НЕКОТОРЫХ ОСОБЕННОСТЯХ ШАЛ, ИНИЦИИРОВАННЫХ ГАММА-КВАНТАМИ ПРЕДЕЛЬНО ВЫСОКИХ ЭНЕРГИЙ

В работе исследуется количество мюонов низких энергий ($E_\gamma \leq$ 1 ГэВ) в ШАЛ, инициированных первичными гамма-квантами предельно высоких энергий. Показано, что на больших глубинах ($z \geq 1000$ г/см^2) количество низкоэнергетических мюонов в ШАЛ от гамма-квантов с энергией $E_0 \geq 10^{18}$эВ, такого же порядка, что и в ШАЛ от протонов, в отличие от области энергий $E_0 \sim 10^{15}$эВ, где гамма-ливни являются "мюонобедными". Исследуется влияние эффектов Ландау-Померанчука-Мигдала и взаимодействия первичного фотона с геомагнитным полем на характер развития электромагнитного ливня при энергиях $E_0 \geq 10^{19}$эВ. В случае большого содержания гамма-квантов в первичном космическом излучении ($\gamma/p > 0{,}1$) при интерпретации данных по ШАЛ предельно высоких энергий, этими эффектами нельзя пренебречь.

Ереванский физический институт
Ереван 1990

1. Introduction

The interaction of cosmic rays (CR) of extremely high energies (EHE) with the microwave background radiation 2.7K due to the π-meson photoproduction leads to the so-called Zatsepin-Greisen "cutoff" in the proton spectrum at $E \geq 5 \cdot 10^{19}$eV. The secondary products of π-meson decays initiate relativistic electron-photon showers in the intergalactic medium, which results in formation of a hard spectrum of diffuse gamma-radiation. The γ/p flux ratio in the energy range $E \geq 5 \cdot 10^{19}$eV, under certain assumptions on the value of the intergalactic magnetic field and the spectrum of the universal radio background, can reach values ~10% [1,2,3]. A high contribution to the diffuse gamma-radiation of extremely high energies can make also the extragalactic sources, in particular, active galaxies in the Local Supercluster [4], which are considered as potential sources of EHE CR at $E \geq 10^{19}$eV (see Ref.[5]).

So, the γ/p ratio contains a direct information about the origin of CR, and the possibility of an experimental measurement of the γ/p ratio at energies $E \geq 10^{19}$eV seems very valuable.

All large air shower arrays for detection of EHE cosmic radiation are designed to measure the characteristics of extensive air showers (EAS) initiated by CR protons and nuclei. In principle these installations can be used to detect EAS from EHE gamma-rays taking into account the peculiarities of development of electromagnetic showers. However, the characteristics of the EAS initiated by EHE gamma-rays are practically not investigated. Meanwhile, there are expected remarkable qualitative changes in the character of electromagnetic EAS development in this energy range.

In this paper we study the content of the low energy (E ~GeV) muons in EAS initiated by primary photons at

$E_0 \geq 10^{18}$eV as well as the influence of the Landau-Pomeranchuk-Migdal (LPM) effect and of the effect of interaction of the primary photons with the geomagnetic field on the EAS development at extremely high energies.

2. Low-Energy Muons in EAS Initiated by EHE Gamma-Rays

The differential spectrum of cascade gamma-rays from an incident primary photon with energy E_0 at a depth z is given in the form [6]

$$F^{\gamma}(E_0,E,z) = \frac{1}{2\pi i}\int_{-i\infty}^{+i\infty}\frac{E_0^s}{E^{s+1}}\,H_{\gamma}(s)\,e^{\lambda_1(s)z/\lambda_R}\,ds\,, \qquad (1)$$

where λ_R is the radiation length equal to 37.1 g/cm^2 in the Earth's atmosphere; the function $H_{\gamma}(s)$ is tabulated in Ref.[6].

In the gamma-induced showers the main contribution to the low-energy muon production make the decays of the photoproduced charged pions. The differential spectrum of pions produced in photomeson processes at a depth of z, has the form:

$$F^{\pi}(E_0,E,z) = \frac{1}{\lambda_{\gamma A}}\int_E^{E_0} F^{\gamma}(E_0,E',z)\;p_{\gamma\pi}(E,E')\;dE' \simeq$$
$$\simeq \frac{2}{\lambda_{\gamma A}}\int_E^{E_0} F^{\gamma}(E_0,E',z)\,\frac{dE'}{E'}\,. \qquad (2)$$

In the Eq.(2) $\lambda_{\gamma A}\simeq\frac{2.4\cdot10^4}{\sigma_{\gamma A}(\mathrm{mb})}(\mathrm{g/cm^2})$, where $\sigma_{\gamma A}$ is the total cross section of photoproduction of $\pi^{\pm}$-mesons. In photonuclear reactions at $E_{\gamma}\leq$2GeV the main contribution makes the pion production. Further on we assume that the $\pi^{\pm}$ photoproduction cross section remains constant in the whole energy range and amounts to $\sigma_{\gamma A}\simeq$2mb. In reality the accelerator data indicate a weak logarithmic growth of the pion photoproduction cross section. But the growth becomes essential only at extremely high energies, remaining considerably smaller than the e^+e^- pair photoproduction cross section (≃500mb). That is why the shower development will be as before determined by the electromagnetic processes, while the production of low-energy

pions (hence of muons) is predominantly due to cascade gamma-quanta with $E_\gamma \le 10$GeV. Consequently, our approximation $\sigma_{\gamma A} \simeq 2$mb seems correct. The production spectrum of muons with energy $E \le 10$GeV, which are due to the pion decay, is [7]

$$F^{\gamma\pi\mu}(E_0,E,z) \simeq \alpha_\pi \int_{E_\pi^-}^{E_\pi^+} F^{\gamma\pi}(E_0,E',z)\,\frac{dE'}{E'}\,, \qquad (3)$$

where

$$\alpha_\pi = \frac{m_\pi^2}{m_\pi^2 - m_\mu^2}\,; \qquad E_\pi^\pm = \frac{m_\pi}{m_\mu}\,\frac{E_\mu E_\mu^* \pm c^2 p_\mu p_\mu^*}{m_\mu c^2}\,.$$

With regard to Eqs.(1) and (2) the Eq.(3) is reduced to

$$F^{\gamma\pi\mu}(E_0,E,z) \simeq \frac{2\alpha_\pi}{\lambda_{\gamma A}}\,\frac{1}{2\pi i}\int_{-i\infty}^{+i\infty}\int_{E_\pi^-}^{E_\pi^+}\frac{E_0^s}{E'^{s+1}}\,\frac{H_\gamma(s)}{(s+1)}\,e^{\lambda_1(s)z/\lambda_R}\,\frac{dE'}{E'}\,ds =$$

$$\frac{2\alpha_\pi}{\lambda_{\gamma A}}\,\frac{1}{2\pi i}\int_{-i\infty}^{+i\infty}\frac{E_0^s}{E^{s+1}}\,\frac{H_\gamma(s)}{(s+1)^2}\,e^{\lambda_1(s)z/\lambda_R}\left[\frac{m_\mu}{m_\pi}\right]^{s+1}\left[\frac{1}{(\chi_\pi^-)^{s+1}} - \frac{1}{(\chi_\pi^+)^{s+1}}\right]ds \qquad (4)$$

In the Eq.(4) $\chi_\pi^\pm = \frac{E_\mu^* \pm p_\mu^* c}{m_\mu c^2}$; $E_\mu^* = 109.8$MeV; $p_\mu^* = 29.8$MeV/c. Noticing that $\frac{m_\mu}{m_\pi}\,\frac{1}{\chi_\pi^-} \approx 1$ and $\frac{m_\mu}{m_\pi}\,\frac{1}{\chi_\pi^+} \approx \frac{1}{2}$, eventually we obtain:

$$F^{\gamma\pi\mu}(E_0,E,z) \simeq \frac{2\alpha_\pi}{\lambda_{\gamma A}}\,\frac{1}{2\pi i}\int_{-i\infty}^{+i\infty}\frac{E_0^s}{E^{s+1}}\,\frac{H_\gamma(s)}{(s+1)^2}\,e^{\lambda_1(s)z/\lambda_R}\left[1 - \frac{1}{2^{s+1}}\right]ds = \qquad (5)$$

$$= \frac{2\alpha_\pi}{\lambda_{\gamma A}}\,\frac{1}{2\pi i}\int_{-i\infty}^{+i\infty} K(s)\,e^{\lambda_1(s)z/\lambda_R}\,ds\,,$$

where $K(s) = \frac{E_0^s}{E^{s+1}}\,\frac{H_\gamma(s)}{(s+1)^2}\left[1 - \frac{1}{2^{s+1}}\right]$. The muon, formed in the pion decay, decays with a probability of $1/(\gamma_\mu E z)$ (reduced to $1\,g/cm^2$), where $\gamma_\mu^{-1} = m_\mu c^2 h_0/(c\tau_\mu)$; τ_μ is the lifetime of muon; h_0 is the scale parameter of atmosphere, $h_0 = z/\rho$ ($h_0 \simeq 6.3$km at the upper atmosphere, and $h_0 \simeq 8.4$km at the sea level), hence, the muon flux is defined as

$$\frac{df}{dz} = -\frac{f}{\gamma_\mu E(z) z} \cdot \qquad (6)$$

On the other hand, the muon loses a fraction of its energy in ionization, bremsstrahlung, pair production and nuclear interactions. Taking into account that in the energy range E≤10GeV the ionization losses dominate, and the approximately constant ones ($k_\mu \simeq 2$MeV cm^2/g), we obtain $E(z)=E(z_0)+k_\mu(z_0-z)$, where z is the depth at which muon with E(z) is produced, z_0 is the depth of observation of the muon with energy $E(z_0)$. Consequently, the probability for the muon produced at the depth z_1 to reach the depth z_0 with energy E, is:

$$\omega(z_1, z_0; E) = \left[\frac{z_1}{z_0}\,\frac{E}{E+k_\mu(z_0-z_1)}\right]^{\frac{1}{\gamma_\mu(E+k_\mu z_0)}}, \qquad (7)$$

where $E \equiv E(z_0)$.

Hence, the muon flux at energy E at the depth z_0 is:

$$F^{\gamma n \mu}(E_0, E, z_0) \simeq \frac{2\alpha_\pi}{\lambda_{\gamma A}}\,\frac{1}{2\pi i}\int_0^{z_0}\int_{-i\infty}^{+i\infty} K(s)\, e^{\lambda_1(s)z'/\lambda_R} \times \qquad (8)$$

$$\times \left[\frac{z'}{z_0}\,\frac{E}{E+k_\mu(z_0-z')}\right]^{\frac{1}{\gamma_\mu(E+k_\mu z_0)}} ds\,dz' \,.$$

The analytical calculation of Eq.(8) is presented in the Appendix. Relatively simple expressions of the differential and integral spectra of low-energy muons in the atmosphere are given by Eqs.(A.7)-(A.12).

Fig.1 shows the number of muons $N_{\gamma\mu}(\geq 0.3\text{GeV})$ as a function of the depth (z) for energy of primary photon $E_0=10^{18}$eV. For comparison the relevant dependence of $N_{p\mu}(\geq 0.3\text{GeV})$ for EAS initiated by primary protons with $E_0=10^{18}$eV, obtained by McComb et al. [8], is also presented. In the same figure we also show the number of muons with energy E≥0.3GeV from primary protons at the sea level, calculated by Dedenko [9]. As it is seen from Fig.1, there is a difference (by a factor of ~2) in the estimates of N_μ obtained in Refs.[8] and [9]. Unfortunately, it is difficult to understand the reason for this divergence, as

the calculations have been carried out numerically. But even with account of this uncertainty of the muon number in proton-induced showers we can claim that the number of low-energy muons in photon-induced showers at $E_0 \geq 10^{18}$eV is at least not less than the number of muons in the proton-induced shower. Note that in our calculations we used the "ordinary" cross section of the $\pi^{\pm}$-meson photoproduction, assuming that the character of the interaction of gamma-rays at extremely high energies did not change dramatically. At the first glance this result seem a strange one, since it is known that in the energy range of $E_0 \sim 10^{15}$eV the number of muons with energy E>1GeV in the gamma-shower in the frames of the standard consideration of the π-meson photoproduction cross section does not exceed 3% of the number of muons in the proton showers (see, e.g. [10-12]). However, the energy ranges of both primary photons ($\geq 10^{18}$eV) and of the shower muons (E≥0.3GeV), as well as large depth of observation ($z_0 \geq 1000 g/cm^2$) are a matter of principle in the case considered. The number of muons in gamma-showers is proportional to the initial energy, while in the proton showers $N_{\mu} \sim E_0^{0.8 \div 0.9}$ [8,13]. At the incident particle energy increasing from 10^{15} to 10^{18}eV, the difference in these dependences leads to the increase of the ratio $N_{\gamma\mu}/N_{p\mu}$ by a factor of about 3-4. The energy range of the detected muons is also very essential, as the muon spectra in the gamma- and proton-induced showers are essentially different. This is seen in Fig.2, which presents the differential spectra (times the energy) of muons from incident gamma-rays and protons at the sea level. The muon spectrum in the proton shower is taken from Ref.[8]. The muon spectrum in the gamma-shower is noticeably steeper than that in the proton shower, and in the energy range of E≤1GeV it goes essentially higher than the muon spectrum in the proton shower. It should be noted that the muons in the proton shower consist of two components - muon from the decay of $\pi^{\pm}$-mesons produced at hadron(nucleon and pion)-air-nuclei interactions, and muons from the decay of $\pi^{\pm}$-mesons produced in photonuclear reactions (in terms of the authors of Ref.[8] - "normal" and "photoproduced" muons, respectively). At energies E<1GeV, as it follows from the calculations of Ref.[8], the

"photoproduced" muons related directly with the electromagnetic branch of the cascade, dominate over the "normal" ones (see Fig.2), this qualitatively agreeing to our conclusions.

It is important to note that the effect mentioned (the approximately equal number of low-energy muons in gamma and proton showers) occurs at large depths ($z \geq 10^3 g/cm^2$), where the number of cascade gamma-rays with $E_\gamma \geq 0.5GeV$ able to produce μ-mesons with energy $E \geq 0.3GeV$ reaches such a value that compensates for the difference (by two orders of magnitude) in the cross sections of the π-meson production by photons and hadrons. To demonstrate this effect qualitatively, let us estimate the number of muons in the gamma-showers of extremely high energies by a simple procedure suggested by Halzen [14].

It is known that the probability of photons absorption due to e^+e^- pair production per radiation length, λ_R, is $\omega_p = 7/9$. In matter the electron is absorbed due to the bremsstrahlung as $E = E_e \exp(-z/\lambda_R)$, where E_e is the initial electron energy. Hence the gamma-quantum is absorbed at a pathlength of $(9/7)\cdot\lambda_R$, and the electron produces a bremsstrahlung gamma-quantum with energy $\sim E_e/2$ at a pathlength of $z = \lambda_R \ln 2$, the electron energy decreasing by a factor of 2. If taken into account that in the electron-photon cascade the $e^\pm$ electrons constitute about the 2/3 of the total number of the cascade particles, and the gamma-rays - the 1/3, then we can introduce the mean pathlength for the cascade particle (electron or photon) in the following form:

$$\langle\lambda\rangle \approx \frac{1}{3}\,\frac{9}{7}\,\lambda_R + \frac{2}{3}\,\ln 2\,\lambda_R \qquad (9)$$

In this case the number of cascade particles ($e^\pm$ and γ) initiated by primary photon with energy E_0 at a depth of z will be 2^n ($n = z/\langle\lambda\rangle$), the mean energy $\langle E\rangle = E_0 2^{-z/\langle\lambda\rangle}$, and the depth of the cascade maximum for particles with energy E_{th} $z_{max} \approx \langle\lambda\rangle \frac{\ln(E_0/E_{th})}{\ln 2}$ (the number of particles at maximum, $N_{max} \approx E_0/E_{th}$). The number of low-energy muons at a given depth is [14]:

$$N_{\gamma\mu} \approx 2R_\gamma\, N_\gamma\ , \qquad (10)$$

where the factor 2 accounts for the contribution of the muons produced at all the previous depths; R_γ is the ratio of the

pion photoproduction cross section to the e^+e^- pair production cross section in air: $R_\gamma=\sigma(\gamma\to\pi X)/\sigma(\gamma\to e^+e^-)\approx 3\div 4\cdot 10^{-3}$. It should be noted that at large depths the probability of $\pi^\pm$ decay (before interaction) decreases due to increase of the air density. In particular, at $z\geq 800 g/cm^2$ the production of muons with energy $E_\mu\geq 20GeV$ via $\pi^\pm$-decays is suppressed. In this energy range of muons the main contribution comes from $K^\pm$-mesons, the production cross section of the latters being by about a factor of 10 less than that of $\pi^\pm$ production. At energies $E_\mu\geq 200GeV$ direct $\mu^\pm$ production becomes dominating. In this energy range $\sigma(\gamma\to\mu^+\mu^-)/\sigma(\gamma\to e^+e^-)\approx 2\cdot 10^{-5}$. Note that this procedure describes the dependence of the number of cascade gamma-rays, and consequently, of the muons correctly at $z\geq z_{max}$. On the other hand, at $z_0>z_{max}$ it is necessary to take into account the muon energy losses. So, let us estimate the number of muons at the depth of $z_0\sim z_{max}$, where the approximation mentioned is relatively correct. At the sea level ($z_0=1030 g/cm^2$) the number of photons from the primary photon with $E_0=10^{18}eV$ approximately is:

$$N_\gamma = \frac{1}{3}\,2^n \approx 7\cdot 10^8; \qquad (n=z_0/\langle\lambda\rangle\approx 31) \qquad (11)$$

As at this depth the gamma-rays mean energy $\langle E_\gamma\rangle\approx E_0/2^n\approx 0.5GeV$ ($z_{max}\approx 10^3 g/cm^2$), and to the muons is transferred ≈ 0.6 fraction of the photon energy (through production and decay of $\pi^\pm$), then substituting the values of R_γ and N_γ into the Eq.(10), we obtain the number of muons with energy $E\geq 0.3GeV$:

$$N_{\gamma\mu} \approx 4\cdot 10^6 \qquad (12)$$

This estimate agrees to the results of the analytical calculations for $z_0=1000 g/cm^2$ (see Fig.1).

Thus, both the analytical solution and the qualitative consideration show, that at $z_0\sim 1000 g/cm^2$ the number of muons with $E_\mu\geq 0.3GeV$ from initial gamma rays with $E_0=10^{18}eV$ is about $N_{\gamma\mu}\approx 4\cdot 10^6$. The relevant number of muons from a proton shower is $N_{p\mu}\approx 2.5\cdot 10^6$ according to [8], and $N_{p\mu}\approx 4.5\cdot 10^6$ according to [9], i.e. at extremely high energies there occurs a complete alignment of the number of low energy muons in the proton and

gamma-showers. Further, the ratio $N_{\gamma\mu}/N_{p\mu}$ slightly increases with the energy of the incident particles. However, starting from $E_0 \geq 10^{19}$eV the character of the development of electromagnetic cascade initiated by primary photon is essentially influenced by two effects - the LPM effect and the effect of e^+e^- pair production by primary photons interacting with the geomagnetic field.

3. The Influence of the LPM Effect and the Effect of Interaction of Primary Photon with the Geomagnetic Field on the Electromagnetic Cascade development in the Atmosphere.

As a rule, in the standard electromagnetic cascade calculations the Bethe Heitler cross section for e^+e^- pair production and electron bremsstrahlung are used. But at extremely high energies, as a result of the LPM effect, the cross sections of these processes in the atmosphere decrease, this leading to a change in the character of the electromagnetic cascade development. The typical energy at which the LPM effect becomes essential, depends on the density of the medium, and in case of the atmosphere is about 10^{18}eV. Taking into account the LPM effect Dedenko [15,16] has investigated the photon-induced electromagnetic cascades in the atmosphere. These calculations show that starting from $E_0 \geq 10^{19}$eV the LPM effect strongly changes the character of the cascade development, in particular, the shower maximum shifts considerably towards the region of $z \geq 1000 g/cm^2$. Figs.3a and 3b show the cascade curves for incident gamma-rays and protons with energy 10^{20}eV and 10^{21}eV, respectively. The cascade curves for incident gamma-rays are presented both with account of the LPM effect and without it (i.e. in the Bethe-Heitler cross section approximation). In case of incident protons the cascade curves are taken from Ref.[15] as well as are plotted based on the phenomenological formula of Gaisser and Hillas [17]. Somewhat different at small depths, these curves are comparable at $z \sim 1000 g/cm^2$. The proton- induced cascade curves are rather close to the photon-induced cascade curve in the Bethe-Heitler cross section approximation. But, as is seen from Figs.3a and

3b, the allowance for the LPM effect strongly suppresses the number of cascade particles. In case of $E_0=10^{20}$eV this cascade curve comes close to the corresponding curves of the proton-induced cascade only at $z\sim1100 g/cm^2$. At the incident particle energy $E_0=10^{21}$eV the photon-induced cascade curve with regard to the LPM effect is by more than an order of magnitude lower than that from the primary protons even at large depths, and the cascade curves from gamma-rays and protons become comparable only at $z\geq1500 g/cm^2$. It is interesting to note that owing to the LPM effect the cascade curve from gamma-rays with $E_0=10^{21}$eV is even lower than the analogous curve at $E_0=10^{20}$eV (see Fig.4). This interesting effect has been first mentioned by Dedenko [16].

Thus, in case of a high content of primary gamma-rays in the EHE CR one should take the LPM effect into account, otherwise the energy of photon-induced showers would be essentially underestimated. This refers especially to the installations measuring the energy of showers by the number of cascade particles on a given level. As it is seen from Figs.3a and 3b, even the installations located at the sea level, may measure the gamma-shower energy correctly only for showers incident at large zenith angles, namely, $\theta\geq30^o$ for $E_0=10^{20}$eV, and $\theta\geq50^o$ for $E_0=10^{21}$eV. However, for showers with large angles of incidence another effect compensating for the LPM effect becomes essential, namely, the interaction of the primary gamma-rays with the geomagnetic field. At energies $E_\gamma\geq5\cdot10^{19}$eV, depending on the direction of primary gamma-rays, the latter effectively interact with the Earth's geomagnetic field, producing e^+e^- pairs. The photon attenuation coefficient in a homogeneous magnetic field depends on the parameter $\varkappa=\frac{1}{2}(E_\gamma/mc^2)(B_\perp/B_{cr})$ ($B_{cr}=4.4\cdot10^{13}$G; $B_\perp$ is the magnetic field component perpendicular to the direction of the photon) [16]:

$$\frac{dW}{dx}\simeq 0.08\,\frac{\alpha}{\lambda_e}\,\frac{B_\perp}{B_{cr}}\,\frac{1}{\varkappa}\,K^2_{1/3}(2/(3\varkappa)) \quad , \qquad (13)$$

where $K_{1/3}$ is the modified Bessel function; $\alpha=1/137$; $\lambda_e=\frac{\hbar}{mc}=3.86\cdot10^{-11}$cm. The dimensionless function $\phi=\frac{1}{\varkappa}K^2_{1/3}(2/(3\varkappa))$ has a maximum at $\varkappa\sim6$ and amounts to $\phi\sim0.62$. In this case the free

path of gamma-rays is minimal:

$$\Lambda_{\pm} = \left(\frac{dW}{dx}\right)^{-1} \approx 4.7\cdot 10^{6} \left(\frac{B_{\perp}}{1G}\right)^{-1} \text{cm} .$$

In the two limits of $\varkappa \gg 1$ and $\varkappa \ll 1$

$$\Lambda_{\pm} = \begin{cases} 7.8\cdot 10^{5}(B_{\perp}/1G)^{-1}\ \varkappa^{1/3}\text{cm}, & \varkappa \gg 1, \\ 1.2\cdot 10^{6}(B_{\perp}/1G)^{-1}\ \exp[4/3\varkappa]\text{cm}, & \varkappa \ll 1. \end{cases} \qquad (14)$$

In particular, for the typical values of the geomagnetic field $B_{\perp}\sim 0.4$ G and of the incident photon energy $E_{\gamma}\sim 10^{20}$eV, the parameter $\varkappa\sim 1$ and correspondingly, the free path of the gamma-rays $\Lambda_{\pm}\sim 10^{6}$cm, which is three orders of magnitude smaller than the typical scale of the Earth's geomagnetic field variation. Though for more correct estimates one should take the dipole character of the geomagnetic field into account, nevertheless this estimate shows qualitatively that gamma-rays with $E_{\gamma}\geq 10^{20}$eV may be effectively absorbed in the geomagnetic field, depending on the angle of incidence. McBreen and Lambert have first paid attention to this important effect [19]. But in the geomagnetic field there does not occur a simple absorption of gamma-rays. The secondary electrons interacting with the magnetic field produce high-energy photons through synchrotron radiation. The latters produce again $e^{+}e^{-}$ pairs, etc. In other words, in the magnetic field there can be developed cascade which are analogous to the electromagnetic cascade in matter. But in this case there is an essential difference lying in the fact that the free path of the next-generation photons having lower energies sharply (exponentially) increases (see Eq.(14), while due to the lack of a threshold of the synchrotron radiation the electrons promptly lose their energy. In other words, in the magnetic field the cascade proceeds effectively up to $\varkappa \sim 1$, then the whole initial energy is transferred into the photon beam. Fig.5 shows the histogram of the distribution of the gamma rays produced in the geomagnetic field prior to impinging on the Earth's atmosphere. The Monte-Carlo calculations have been carried out for the primary photon energies $E_{\gamma} = 5\cdot 10^{19}$; 10^{20} and 10^{21}eV, and for the magnetic field component perpendicular to the incident photon direction,

$B_{\perp}$=0.4 G. In the calculations the geomagnetic field was supposed to have a dipole character up to distances $R \sim 5R_E$ (R_E is the Earth's radius). Electron deflection in magnetic field was ignored, as at energies $E_e \geq 10^{15}$eV $\theta = \frac{\Delta R}{R_L} = \frac{\Delta R}{pc} eH \leq 10^{-5}$.

The calculations have shown that practically the whole energy of incident photons (≥99.9%) as a result of cascade in the geomagnetic field is redistributed between the cascade gamma-rays with energies $E_\gamma \geq 10^{15}$eV (see Fig.5), the shape of the photon distribution depending on the initial energy weakly. As all the photons in the beam impinging on the Earth's atmosphere initiate EAS, and the LPM effect being suppressed for them (the main fraction of the beam photons have energies $E_\gamma \leq 10^{19}$eV), the superposition of these showers will qualitatively imitate EAS from the primary photon incident directly on the atmosphere, but with no account of the LPM effect. Figs.3a and 3b show cascade curves from superposition of the EAS initiated by the beam of photons produced in the geomagnetic field. The comparison of these curves with the curve of the cascade initiated by the primary photon interacting directly with the atmosphere shows, that the cascade curve from the beam of photons climbs higher, and at $z \approx 800 g/cm^2$ reaches the cascade curves of the primary protons of corresponding energies. In other words, the effect of the photon beam formation in the geomagnetic field "switches" the LPM effect. So, in case of interaction of the incident gamma-rays with the geomagnetic field, the cascade curve from a photon beam coincides formally with that from an individual primary photon directly interacting with the Earth's atmosphere, calculated in the Bethe-Heitler approximation. However, this statement is valid only for $z \geq 800 g/cm^2$. For smaller depths the cascade curve from a photon beam goes considerably higher (see Fig.3). This is explained by the fact that the low-energy photons ($E_\gamma \sim 10^{15} \div 10^{17}$eV) of the beam initiate showers, the maximum of which is achieved at small depths in the atmosphere.

4. Discussion

One of the principal problems of the modern ground-based gamma-ray astronomy spanning very high ($E \geq 1$TeV), ultrahigh ($E \geq 1$PeV) and extremely high ($E \geq 1$EeV) energies, is the development of effective methods for photon-induced shower identification. In case of discrete sources these methods essentially improve the sensitivity of the detectors. Besides, the effeptive methods of rejection of the CR shower background allow to separate the so-called diffuse component of primary gamma-radiation. In the EHE region, identification of the gamma- and nucleon-induced showers is of a special importance, since in that energy range along with gamma-rays there are also expected other neutral particles from discrete galactic sources, namely, neutrons, the pathlength of which (until the decay) at $E \geq 10^{18}$eV is comparable with the radius of the galactic disc, $d = 10(E/10^{18}\text{eV})$kpc. For instance, the EHE signal from the X-ray binary Cyg X-3, which was reported recently by several independent groups [20,21,22], may be associated with both primary photons and neutrons.

In the UHE range the most reliable criterion of separation of the gamma- and proton-induced showers is the muon content in the cascade, provided the character of interaction of gamma-rays with matter is not changed dramatically. However, in the EHE range, even without the last condition, the "muon poorness" criterion becomes inefficient. The calculations carried out in section 1 show that the low-energy ($E_\mu \leq 1$GeV) muon content in the EHE gamma- and proton-induced showers ($E \geq 10^{18}$eV) at large depths of observation ($z \sim 1000 g/cm^2$) become comparable. This is due to the high penetrability of the low-energy ($E_\gamma \sim 1$GeV) photons in an EHE electromagnetic cascade. As a result, at large depths the difference of the cross sections of the $\pi^{\pm}$-meson photoproduction (in gamma-showers) and hadroproduction (in proton showers) is compensated by the photon number in the electromagnetic cascade, which much exceeds the number of hadrons in a proton-induced shower. At the same time, the ratio $N_{\gamma\mu}/N_{p\mu}$ cannot be essentially larger than unity, since in a hadronic cascade there always exists the

electromagnetic branch from the π^0-mesons produced in the initial act (the latters bear about 15% of the initial proton energy).

It is important to emphasize that the claim on a high muon content in the gamma-showers is valid only for low energy muons ($E_\mu \leq 1$GeV). As the muon spectrum in the gamma showers is considerably steeper than the muon spectrum in the proton shower, the gamma-showers remain poor of high-energy muons as before. Therefore, the high-energy muons ($E_\mu \geq 10$GeV) are more informative for identification of the gamma-shower, and combination of low-energy and high-energy muon detectors in EAS arrays seems advantageous. The muon flux measurement at two different energies will allow to get information on the muon spectrum and thus to improve the reliability of identification. Besides, the number (or the density) of muons is used to estimate the energy of primary particles, as it is done, in particular, at the Haverah Park. However, such an estimation procedure without a preliminary identification of primaries, may lead to incorrect estimates of the initial energy. In particular, the gamma-ray-induced shower energy estimation based on low-energy muon data in accordance with the procedure valid for the proton showers, may lead to overestimation of the incident particle energy. The overestimation may be particularly substantial in case of using the parameter ρ (the muon density at large distances from the axis of the shower), as it is expected that owing to the steeper spectrum of the muons in the gamma-showers the ratio $\rho_{\gamma\mu}/\rho_{p\mu}$ for the low-energy muons at large distances may be still larger than the ratio $N_{\gamma\mu}/N_{p\mu}$. However, for firmer claims we need detailed calculations of both hadron and electromagnetic cascades at extremely high energies. Such calculation seems important from the viewpoint of an analysis of the EAS data obtained at different shower installations in the energy range of the so-called "black-body cutoff" ($E \geq 5 \cdot 10^{19}$eV), where the gamma-ray content of the CR may reach a rather large value ($\geq 10\%$) [1-4].

But in this energy range the development of the gamma-ray-induced shower strongly depends on two factors - the LPM effect and the effect of interaction of primary photon with

the geomagnetic field. As it is seen from Figs.3a and 3b, the LPM effect at $E_0 \geq 10^{19}$eV leads to a strong suppression of electromagnetic cascades in the atmosphere up to depths $z \geq 1000 g/cm^2$. Hence it is obvious that the shower energy determination by an installation which detects the number and density of the cascade particles on a given observation level, may lead to a strong underestimation of the EAS energy, if the LPM effect is not taken into account. It is visualized in Fig.4, which presents the cascade curves from incident gamma-rays with energies 10^{20}eV and 10^{21}eV. The LPM effect brings to the fact that the cascade curve from photons with $E=10^{21}$eV up to depths $z \sim 1000 g/cm^2$ is lower than that with $E=10^{20}$eV. So, to identify the EHE photon showers, one should reconstruct the cascade curve, which is possible to do with the help of an installation of the Fly's Eye type. A distinctive feature of these curves is their monotonous growth with z (up to $z \sim 1500 g/cm^2$), hence the shape of the cascade curve may in principle serve as a good criterion for a gamma-shower selection. It should be noted that the cascade curve sections corresponding to large depths ($z \geq 1000 g/cm^2$) are most informative, which automatically means a wide angle of incidence of the primary particles. For instance, for the Fly's Eye installation the zenith angle of incidence must be $\theta \geq 30^o \div 40^o$.

However, for large zenith angles, when the detectors are installed at middle latitudes, the primary gamma-rays with $E \geq 3 \cdot 10^{19}$eV begin to interact effectively with the geomagnetic field, this radically changing the character of the electromagnetic cascade development. As a result of interaction of gamma-rays with the geomagnetic field a photon beam is formed, and since the whole energy of the initial gamma-rays is transferred to the photons with energy $E \geq 10^{15}$eV (see Fig.5), the latters, impinging on the atmosphere, initiate EAS. The cascade curve from superposition of these showers is much higher than that in case of a direct incidence of the primary protons on the atmosphere (see Figs.3,4). This is due to the fact that the energy of the beam photons produced in the geomagnetic field is considerably lower (by more than an order

of magnitude) than that of the primary photon, and in case of a photon beam the influence of the LPM effect on the character of the shower development is insignificant.

Thus, in the case the incident photons interact with the geomagnetic field, the LPM effect is "switched off", and we deal with more "normal" cascade curves. That is why the interaction of gamma-rays with the geomagnetic field becomes a matter of principle. For the primary photon with energy $E \geq 3 \cdot 10^{19}$eV to interact efficiently with the geomagnetic field, it is necessary that the condition of $B_{\perp} \geq 0.4$ G be met. At a given geographic location of the installation the perpendicular component of the magnetic field to the direction of the primary particle, is defined as:

$$B_{\perp} = \frac{M}{R^3} (1+3\sin^2\lambda)^{1/2} \cos[\theta - \mathrm{arctg}(B_r/B_t)] , \qquad (15)$$

where M is the magnetic moment of the dipole (in the first approximation the Earth's magnetic field can be represented as a magnetic dipole with a moment of $8.1 \cdot 10^{25}$G$\cdot$cm^3); R is the distance to its centre; B_r and B_t are the radial and tangent components of the magnetic field at a given latitude λ. In Eq (15) we ignore the weak dependence on the azimuth angle, assuming that the axis of the Earth's magnetic field coincides with that of rotation. Fig.6 presents the values of $B_{\perp}$ as a function of the primary particle incidence zenith angle for several latitudes, $\lambda = 0^{\circ}$; 40°; 50°; 90°. Note that the values of $\lambda = 40^{\circ}$ and 55° correspond to the locations of the Haverah Park and the Fly's Eye, respectively. As it is seen from the figure, for these installations the value of $B_{\perp}$ reaches $B_{\perp} \geq 0.4$ G at zenith angles $\theta \geq 30^{\circ}$. Then, if there really exist gamma ray fluxes with $E \geq 3 \cdot 10^{19}$eV, then these installations will detect them as showers with energy $E \geq 3 \cdot 10^{19}$eV only when $\theta \geq 30^{\circ}$ (at a "standard" data handling, which supposes that all the showers are initiated by incident protons or nuclei). In case of $\theta < 30^{\circ}$, due to an incomplete cascade development at $z_0/\cos\theta$, and as a result of the influence of the LPM effect, the primary particle energy will be underestimated substantially. Whereas at $\theta \geq 30^{\circ}$, due to interaction of primary photon with the geomagnetic

field, the cascade initiated by the beam gamma-rays in the atmosphere regains its "normal" form. And what is more, in this case, if the low-energy muon density is used to determine the shower energy at large distances from the shower axis (as it is done , e.g at the Haverah Park), then a considerable overestimation of the shower energy is possible. This is due to the fact, that more than 80÷90% of the incident photon energy, after interaction with the magnetic field is transferred to secondary photons with $E \geq 10^{18}$eV, which in their turn initiate showers which are rich of low-energy muons at large depths.

In conclusion we should like to note the necessity of taking into account this quite off-beat interlacing of the effects arising at the development of EAS from incident EHE photons considered in this paper. We think it expedient to carry out a new analysis of EHE EAS data obtained at different installations, taking the effects considered into account. This will allow to get a definite information about the content of EHE gamma-rays in the CR, as well as maybe to understand the reason of the divergent results concerning the CR spectrum at $E \simeq 5 \cdot 10^{19}$eV reported by different groups.

We regret that the untimely death of our friend Valerij Vardanian did not allow him to finish the present work with us.

APPENDIX

Calculation of the Muon Spectra in a Photon-Induced Shower

Since the main contribution to the muon production in Eq.(8) makes the range of $z_{max} \sim \ln E_0/E$, we can factor the probability of the muon "survival" at the point z_{max} outside the integral sign. Then, integrating the Eq.(8) over z' we obtain:

$$F^{\gamma\pi\mu}(E_0,E,z_0) \simeq \frac{2\alpha_\pi \lambda_R}{\lambda_\gamma A}\left[\frac{z_{max}}{z_0}\,\frac{E}{E+k_\mu(z_0-z_{max})}\right]^{\frac{1}{\gamma_\mu(E+k_\mu z_0)}} \times$$

$$\times \frac{1}{2\pi i}\int_{-i\infty}^{+i\infty} K(s)\,\frac{e^{\lambda_1(s)z_0/\lambda_R}-1}{\lambda_1(s)}ds \qquad (A.1)$$

Note that the Eq.(A.1) is valid when $z_0 \geq z_{max}$. When $z_0 < z_{max}$, in Eq.(A.1) the probability of the muon "survival" acquires a value equal to unity. The integral in Eq.(A.1) is easily calculated by the saddle-point method, for instance,

$$\frac{1}{2\pi i}\int_{-i\infty}^{+i\infty} ds \frac{E_0^s}{E^{s+1}}\,\frac{H_\gamma(s)}{(s+1)^2}\,\frac{e^{\lambda_1(s)t_0}-1}{\lambda_1(s)} = \frac{1}{2\pi i}\,\frac{1}{E}\left[\int_{-i\infty}^{+i\infty} ds\, H_\gamma(s) \times\right.$$

$$\times \exp(xs-2\ln(s+1)-\ln(\lambda_1(s))+\lambda_1(s)t_0) - \int_{-i\infty}^{+i\infty} ds\, H_\gamma(s)\exp(xs-2\ln(s+1)-$$

$$\left. - \ln(\lambda_1(s)))\right] \approx \frac{1}{(2\pi)^{1/2}}\left\{\frac{E_0^{s_1}}{E^{s_1+1}}\,\frac{H_\gamma(s_1)}{\lambda_1(s_1)(s_1+1)^2}\,e^{\lambda_1(s_1)t_0}\left[\lambda_1''(s_1)t_0 + \right.\right.$$

$$\left. + \frac{2}{(s_1+1)^2} + \frac{\lambda_1'(s_1)^2-\lambda_1(s_1)\lambda_1''(s_1)}{(\lambda_1(s_1))^2}\right]^{-1/2} - \frac{E_0^{s_2}}{E^{s_2+1}}\,\frac{H_\gamma(s_2)}{\lambda_1(s_2)(s_2+1)^2} \times$$

$$\left. \times \left[\frac{2}{(s_2+1)^2} + \frac{(\lambda_1'(s_2))^2-\lambda_1(s_2)\lambda_1''(s_2)}{(\lambda_1(s_2))^2}\right]^{-1/2}\right\}. \qquad (A.2)$$

where $t_0 = z_0/\lambda_R$, $x = \ln E_0/E$ and s_1, s_2 are defined from the conditions

$$t_0 = -\frac{1}{\lambda_1'(s_1)}\left[\ln\frac{E_0}{E} - \frac{2}{s_1+1} - \frac{\lambda_1'(s_1)}{\lambda_1(s_1)}\right], \ln\frac{E_0}{E} - \frac{2}{s_2+1} + \frac{\lambda_1'(s_2)}{\lambda_1(s_2)}. \quad (A.3)$$

It should be noted that when calculating the integrals in Eq.(A.2) we took into consideration the fact that each integrand was the product of the slightly varying function of s, $H_j(s)$, by the exponential function of the form $\exp[xs-2\ln(s+1)-\ln(\lambda_1(s))+m\lambda_1(s)t_0]$. In Eq.(A.1) the maximum of shower development of particles with energy E is $z_{max}\simeq\lambda_R(\ln E_0/E-1)$. The other integrals in Eq.(A.1) are calculated analogously.

For the differential spectrum of muons at the depth z_0 we obtain :

$$F^{\pi,K\mu}(E_0,E,z_0) \simeq \frac{2+\gamma}{(2\pi)^{1/2}}\frac{\lambda_R}{\lambda_A}\left[\frac{z_{max}}{z_0}\frac{E}{E+k_\mu(z_0-z_{max})}\right]^{\frac{1}{\gamma_\mu(E+k_\mu z_0)}} \cdot \quad (A.4)$$

$$\cdot\left[Q(s_1,z_0)e^{\lambda_1(s_1)\frac{z_0}{R}}R(s_2)\cdot Q(s_3,z_0)e^{\lambda_1(s_3)\frac{z_0}{R}}\frac{1}{\frac{s_3+1}{2}} + \frac{R(s_4)}{\frac{s_4+1}{2}}\right],$$

where

$$Q(s,z_0)\simeq\frac{H_j(s)}{\lambda_1(s)(s+1)^2}\frac{E_0^s}{E^{s+1}}\left[\lambda_1''(s)\frac{z_0}{R}+\frac{2}{(s+1)^2}+\frac{(\lambda_1'(s))^2-\lambda_1(s)\lambda_1''(s)}{(\lambda_1(s))^2}\right]^{-1/2}, \quad (A.5)$$

$$R(s)\simeq\frac{H_j(s)}{\lambda_1(s)(s+1)^2}\frac{E_0^s}{E^{s+1}}\left[\frac{2}{(s+1)^2}+\frac{(\lambda_1'(s))^2-\lambda_1(s)\lambda_1''(s)}{(\lambda_1(s))^2}\right]^{-1/2}.$$

The parameters s_1 and s_2 are defined by Eq.(A.3), and s_3, s_4 are defined from the following conditions:

$$t_0 \simeq \frac{1}{\lambda_1(s_3)}\left[\ln\frac{E_0}{E}-\frac{2}{s_3+1}-\ln 2+\frac{\lambda_1'(s_3)}{\lambda_1(s_3)}\right]; \quad (A.6)$$

$$\ln\frac{E_0}{E}-\frac{2}{s_4+1}+\ln 2+\frac{\lambda_1'(s_4)}{\lambda_1(s_4)}.$$

Here the difference between s_3 and s_1 as well as between s_4

and s_2 is a slight one, then in the first approximation we may assume that $s_1 \approx s_3$ and $s_2 \approx s_4$. Then, for differential spectrum of muons we finally obtain:

$$F^{\gamma n\mu}(E_0,E,z_0) \approx \frac{2\alpha_\pi \lambda_R}{(2\pi)^{1/2}\,\lambda_{\gamma A}} \left[\frac{z_{max}}{z_0}\,\frac{E}{E+k_\mu(z_0-z_{max})}\right]^{\frac{1}{\gamma_\mu(E+k_\mu z_0)}} \times \tag{A.7}$$

$$\times \left[Q(s_1,z_0)e^{\lambda_1(s_1)\frac{z_0}{\lambda_R}}\left(1 - \frac{1}{2^{s_1+1}}\right) - R(s_2)\left(1 - \frac{1}{2^{s_2+1}}\right)\right]$$

for $z_0 \geq z_{max}$, and

$$F^{\gamma n\mu}(E_0,E,z_0) \approx \frac{2\alpha_\pi \lambda_R}{(2\pi)^{1/2}\,\lambda_{\gamma A}} \times \tag{A.8}$$

$$\times \left[Q(s_1,z_0)e^{\lambda_1(s_1)\frac{z_0}{\lambda_R}}\left(1 - \frac{1}{2^{s_1+1}}\right) - R(s_2)\left(1 - \frac{1}{2^{s_2+1}}\right)\right]$$

for $z_0 < z_{max}$. The integral muon flux, $N(E_0,E,z_0) \equiv F(E_0,>E,z_0)$, can be obtained similarly:

$$N^{\gamma n\mu}(E_0,E,z_0) \approx \frac{2\alpha_\pi \lambda_R}{(2\pi)^{1/2}\,\lambda_{\gamma A}} \times \tag{A.9}$$

$$\times \left[Q^0(s_1,z_0)\frac{e^{\lambda_1(s_1)\frac{z_0}{\lambda_R}}}{s_1}\left(1 - \frac{1}{2^{s_1+1}}\right) - \frac{R^0(s_2)}{s_2}\left(1 - \frac{1}{2^{s_2+1}}\right)\right],$$

when $z_0 < z_{max}$, and

$$N^{\gamma n\mu}(E_0,E,z_0) \approx \frac{2\alpha_\pi \lambda_R}{(2\pi)^{1/2}\,\lambda_{\gamma A}} \left[\frac{z_{max}}{z_0}\,\frac{E}{E+k_\mu(z_0-z_{max})}\right]^{\frac{1}{\gamma_\mu(E+k_\mu z_0)}} \tag{A.10}$$

$$\times \left[Q^0(s_1,z_0)\frac{e^{\lambda_1(s_1)\frac{z_0}{\lambda_R}}}{s_1 - \frac{1}{\gamma_\mu(E+k_\mu z_0)}}\left(1 - \frac{1}{2^{s_1+1}}\right) - \frac{R^0(s_2)}{s_2 - \frac{1}{\gamma_\mu(E+k_\mu z_0)}}\left(1 - \frac{1}{2^{s_2+1}}\right)\right],$$

when $z_0 \geq z_{max}$.

$$Q^0(s,z_0)\simeq\frac{H_\gamma(s)}{\lambda_1(s)(s+1)^2}\frac{E_0^s}{E^s}\left[\lambda_1''(s)\frac{z_0}{\lambda_R}+\frac{2}{(s+1)^2}+\frac{1}{\left(s-\frac{\theta(z_0-z_{max})}{\gamma_\mu(E+k_\mu z_0)}\right)^2}+\right.$$

$$\left.+\frac{(\lambda_1'(s))^2-\lambda_1(s)\lambda_1''(s)}{(\lambda_1(s))^2}\right]^{-1/2}. \qquad (A.11)$$

$$R^0(s)\simeq\frac{H_\gamma(s)}{\lambda_1(s)(s+1)^2}\frac{E_0^s}{E^s}\left[\frac{2}{(s+1)^2}+\frac{1}{\left(s-\frac{\theta(z_0-z_{max})}{\gamma_\mu(E+k_\mu z_0)}\right)^2}+\right.$$

$$\left.+\frac{(\lambda_1'(s))^2-\lambda_1(s)\lambda_1''(s)}{(\lambda_1(s))^2}\right]^{-1/2}.$$

s_1 and s_2 are defined from:

$$\frac{z_0}{\lambda_R}=-\frac{1}{\lambda_1'(s_1)}\left[\ln\frac{E_0}{E}-\frac{2}{s_1+1}-\frac{1}{\left(s_1-\frac{\theta(z_0-z_{max})}{\gamma_\mu(E+k_\mu z_0)}\right)}-\frac{\lambda_1'(s_1)}{\lambda_1(s_1)}\right]; \qquad (A.12)$$

$$\ln\frac{E_0}{E}=\frac{2}{s_2+1}+\frac{1}{\left(s_2-\frac{\theta(z_0-z_{max})}{\gamma_\mu(E+k_\mu z_0)}\right)}+\frac{\lambda_1'(s_2)}{\lambda_1(s_2)},$$

where $z_{max}\approx\lambda_R(\ln\frac{E_0}{E}-2)$ and $\theta(z_0-z_{max})=\begin{cases}1, & z_0\geq z_{max}\\ 0, & z_0<z_{max}\end{cases}$

Figure Captions

Fig.1 The number of muons with energy E≥0.3GeV for the primary particle energy $E_0=10^{18}$eV. The solid curve is the analytical solution of Eq.(8) for muons produced in a gamma-induced shower (Eqs.(A.9), (A.10)). The point "o" corresponds to the number of muons in the gamma-induced shower at the sea level, obtained by Halzen's procedure. The dashed curve corresponding to the muon number in the proton-induced shower, is taken from Ref.[8]. The point "×" corresponding to the number of muons in a proton-induced shower at the sea level is taken from Ref.[9].

Fig.2 The differential spectra of muons (times the energy) at the sea level from incident gamma-rays (curve 1) and incident protons (curve 2). The curves 2a and 2b taken from Ref.[8] are the "normal" and the "photoproduced" muons in the proton-induced shower, respectively (2=2a+2b).

Fig.3a,b Cascade curves for incident gamma-rays and protons with energy 10^{20}eV (3a) and 10^{21}eV (3b). In case of incident photons the cascade curves are obtained with account of the LPM effect (---), and with no account of it, i.e. in the Bethe-Heitler approximation (-·-). The curve (-···-) denotes the cascade curve from a gamma-ray beam formed at interaction of the primary photon with the geomagnetic field. For incident protons the cascade curves are taken from Ref.[15] (——), as well as are plotted in terms of the phenomenological formula of Gaisser and Hillas [17] (-o-).

Fig.4 Cascade curves for primary photons 10^{20}eV and 10^{21}eV, both with ($B_\perp$=0.4 G) and without (B=0) account of interaction of gamma-rays with the geomagnetic field.

Fig.5 The Monte-Carlo calculations of energy distribution of gamma-rays formed in the geomagnetic field at interaction of incident photons with energies $5\cdot10^{19}$eV; 10^{20}eV and 10^{21}eV. The magnetic field component perpendicular to the direction of the primary photon $B_\perp$=0.4 G.

Fig.6 The magnetic field perpendicular component $B_\perp$ as a function of the zenith angle of the incident photon at different geographic latitudes.

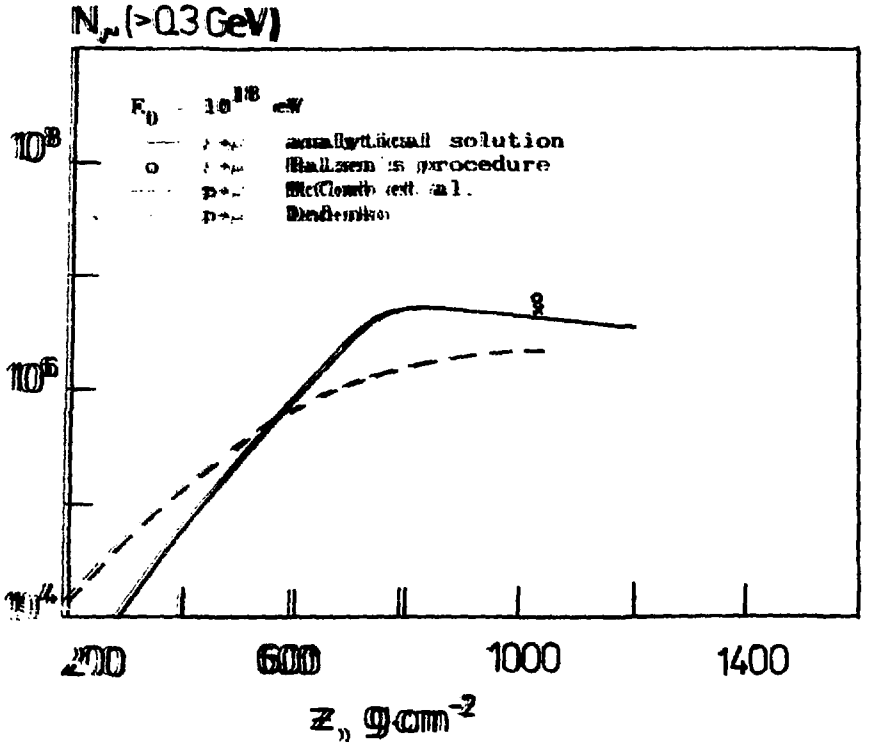
N_μ (>0.3 GeV)
E_0 = 10^{18} eV
analytical solution
Hillas's procedure
McClomb et al.
Dedenko
10^8
10^6
200
600
1000
1400
X_μ, g cm^{-2}

Fig. 1

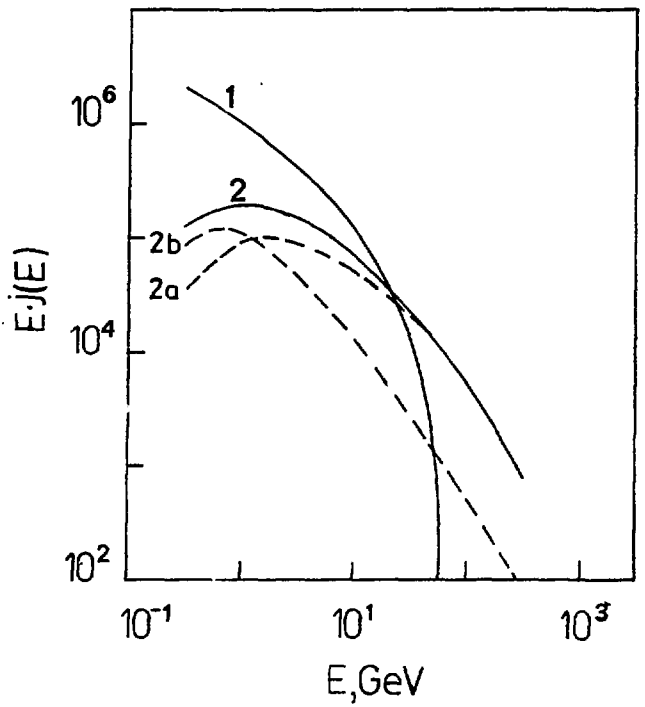

Fig. 2

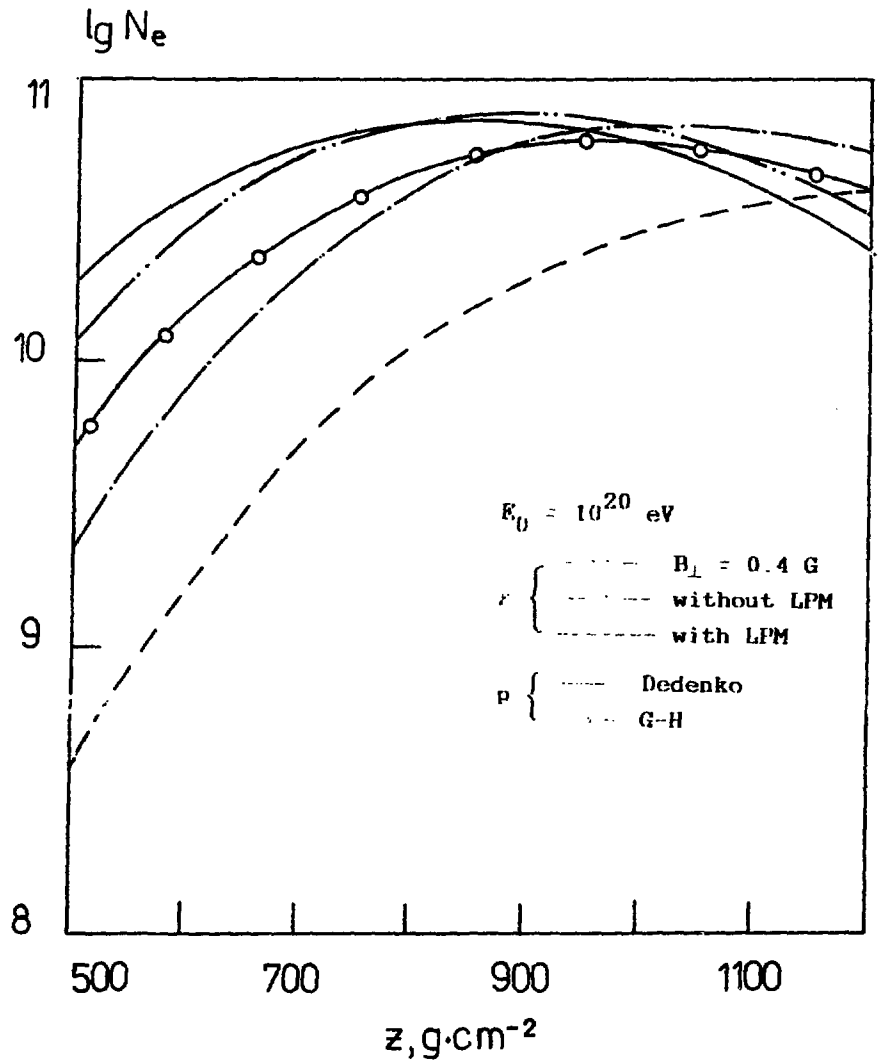
lg Ne
11
10
9
8
500
700
900
1100
z, g·cm⁻²
E0 = 10^20 eV
γ
B⊥ = 0.4 G
without LPM
with LPM
p
Dedenko
G-H

Fig.3a

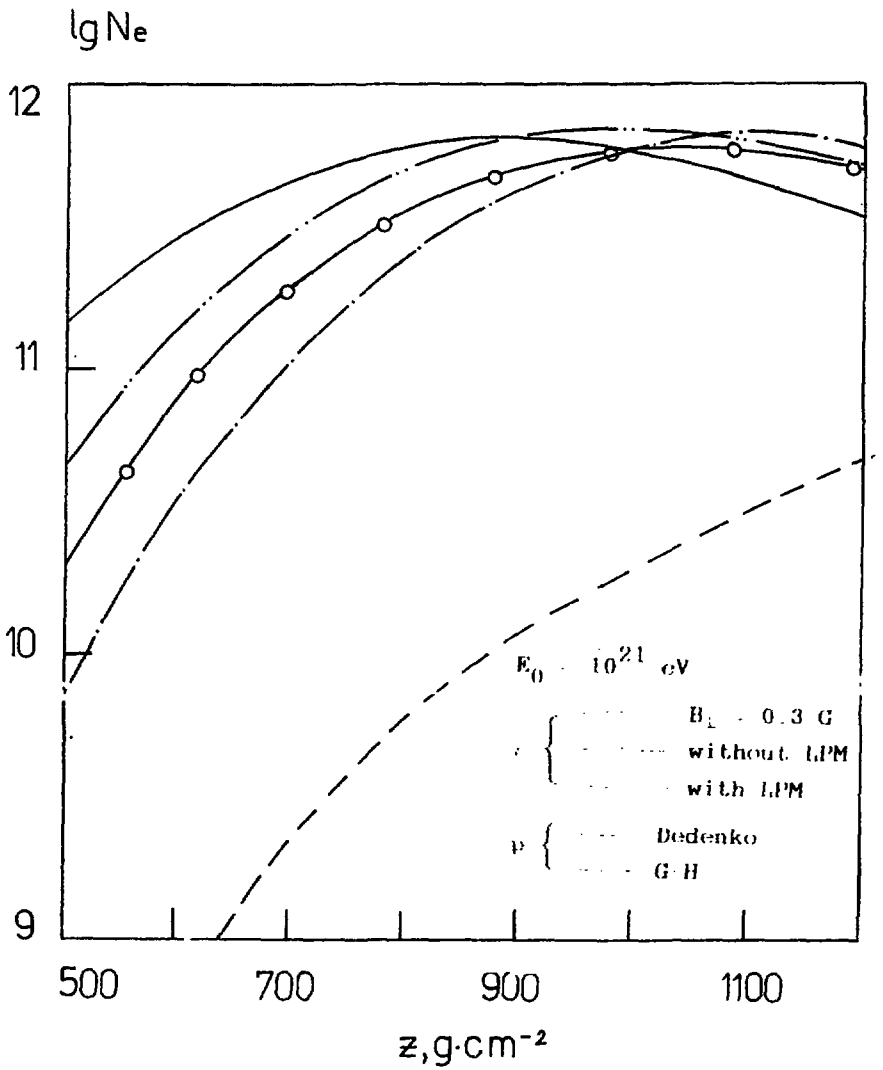
lg Ne
12
11
10
9
500
700
900
1100
z, g·cm⁻²
E0 = 10^21 eV
γ
B⊥ = 0.3 G
without LPM
with LPM
p
Dedenko
G·H

Fig.3b

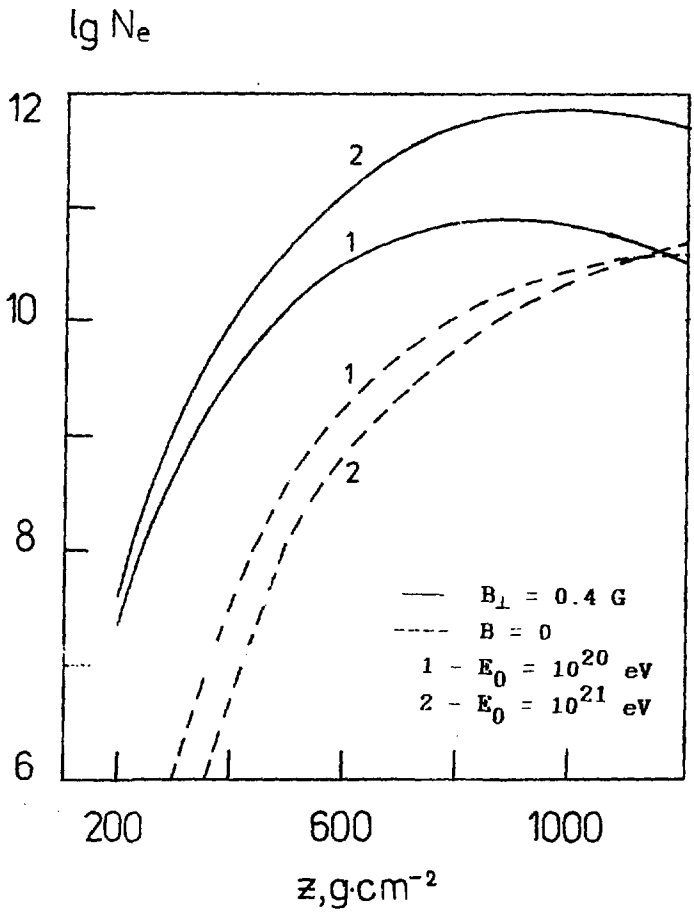
lg Ne
12
10
8
6
200
600
1000
z, g·cm⁻²
2
1
1
2
B⊥ = 0.4 G
B = 0
1 - E0 = 10^20 eV
2 - E0 = 10^21 eV

Fig. 4

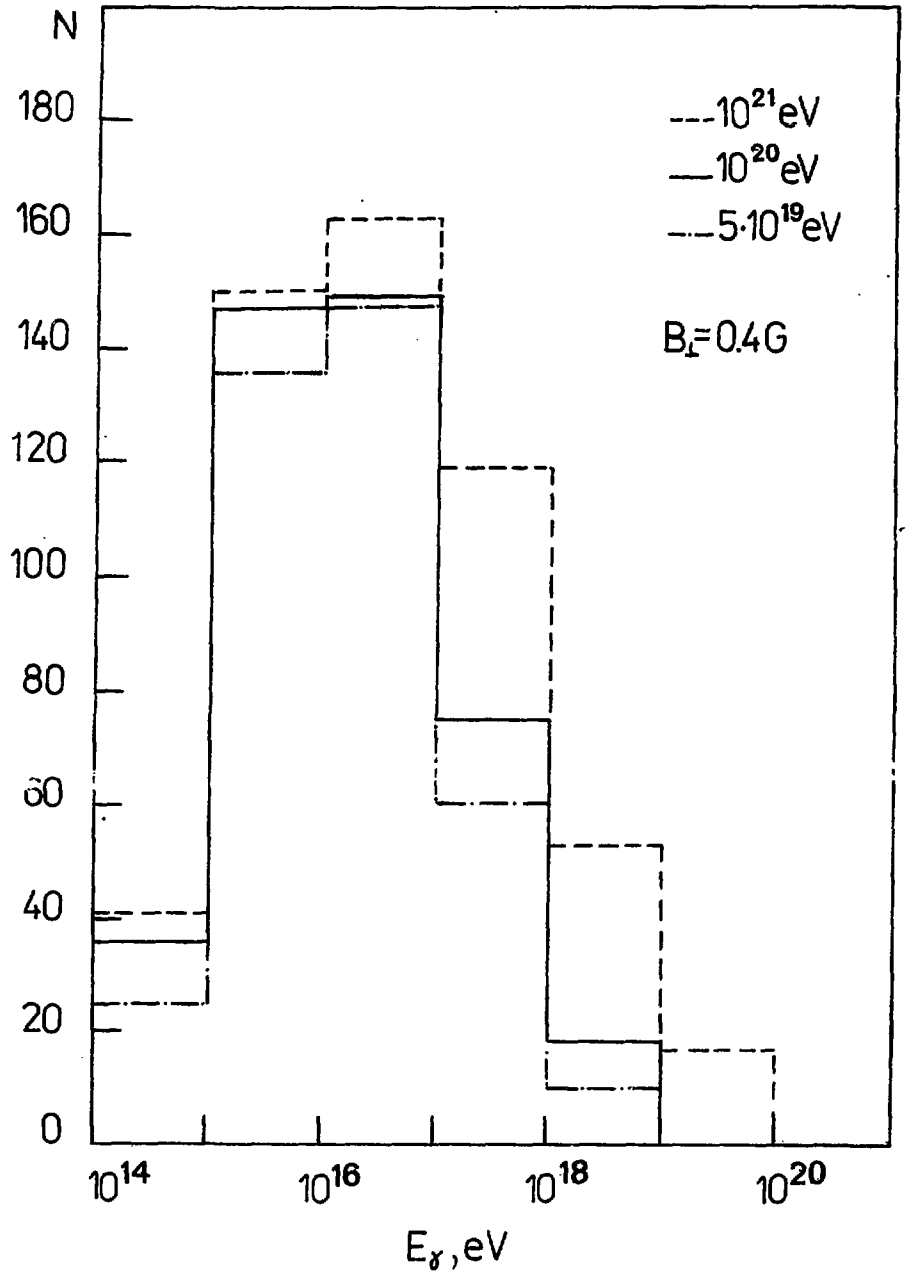
N
180
160
140
120
100
80
60
40
20
0
10^{14}
10^{16}
10^{18}
10^{20}
E_γ, eV
---10^{21}eV
—10^{20}eV
-·-$5\cdot10^{19}$eV
$B_\perp$=0.4G

Fig.5

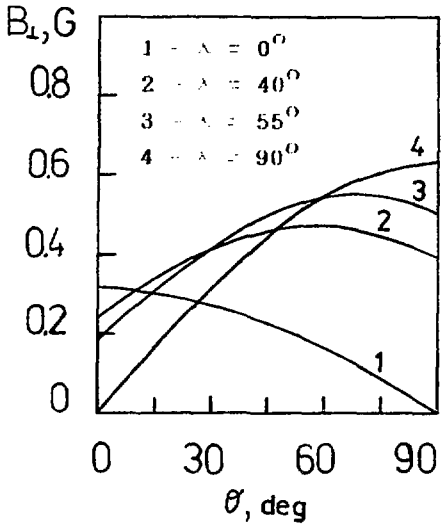

Fig.6

References

1. Wdovczyk J., Tkaczyk W., Wolfendale A.W. J.Phys., 1972, v.A5, p.1419.
2. Aharonian F.A., Kanevsky B.L., Vardanian V.V. Preprint YERPHI-1135(12)-89.
3. Halzen F., Protheroe R.J., Stanev T., Vankov H.P. Preprint MAD/PH/, 470, 1989.
4. Aharonian F.A. Preprint YERPHI, in press, 1990.
5. Berezinsky V.S., Bulanov S.V., Ginzburg V.L. et al. Astrophysics of Cosmic Rays. Moscow, Nauka Pub., 1984.
6. Rossi B., Greisen K. Cosmic Ray Theory. Rev.Mod.Phys., 1941, v.13, No.4, p.240.
7. Hayakawa S. Cosmic Ray Physics. New York, 1969.
8. McComb T.J.L., Protheroe R.J., Turver K.E. J.Phys. G: Nucl. Phys., 1979, v.5, p.1613.
9. Dedenko L.G. Proc. 21st ICRC 1990, v.8, p.248.
10. Stanev T., Gaisser T.K., Halzen F. Phys.Rev., 1985, v.D32, p.1244.
11. Edwards P.G., Protheroe R.J., Ravinski E. J.Phys. G: Nucl. Phys., 1985, v.11, p.101.
12. Procureur J., Stamenev J.N. Proc. 20th ICRC, 1987, v.6, p.24.
13. Matsubara Y., Hara T., Hayashida N. et al. J.Phys. G: Nucl. Phys., 1988, v.14, p.385.
14. Halzen F. Preprint MAD/PH/, 459, 1988.
15. Dedenko L.G. Proc. VHE Gamma Ray Astronomy, Crimea, 1989, p.106.
16. Dedenko L.G., Zheleznikh I.M., Kolomatsky S.P. Izv. Akad. Nauk SSS, ser. Fizicheskaya, 1989, v.53, No.2, p.350.
17. Gaisser T.K., Hillas A.M. Proc. 15th ICRC, 1977, v.8, p.353.
18. Erber T. Rev.Mod.Phys., 1966, v.38, p.626.
19. McBreen B., Lambert C.J. Proc. 17th ICRC, 1981, v.6, p.70.
20. Gassiday G.L., Cooper R., Dawson B.R. et al. Phys. Rev. Lett., 1988, v.62, p.383.
21. Teshima M., Hara T., Hayashida N. Proc. 21st ICRC, 1990, v.3, p.71.

22. Glushkov A.V., Efimov N.N., Efremov N.N. et al. Proc. VHE Gamma Ray Astronomy, Crimea, 1989, p.177.

The manuscript was received July 23, 1990

Ф.А. АГАРОНЯН, Б.Л. КАНЕВСКИЙ, В.А. САКЯН
О НЕКОТОРЫХ ОСОБЕННОСТЯХ ШАЛ, ИНИЦИИРОВАННЫХ ГАММА-КВАНТАМИ ПРЕДЕЛЬНО ВЫСОКИХ ЭНЕРГИЙ
(на английском языке, перевод Г.А. Папяна)
Редактор Л.П.Мукаян
Технический редактор А.С.Абрамян

Подписано в печать 19/X-90 | Формат 60×84×16
Офсетная печать. Уч.изд.л. 1,6 | Тираж 299 экз.Ц.23 к.
Зак.тип. 288 | Индекс 3649

Отпечатано в Ереванском физическом институте
Ереван-36, ул. Братьев Алиханян 2.

The address for requests:
Information Department
Yerevan Physics Institute
Alikhanian Brothers 2,
Yrevan, 375036
Armenia, USSR

ИНДЕКС 3649

ЕРЕВАНСКИЙ ФИЗИЧЕСКИЙ ИНСТИТУТ